Remote Sensing of Environment 115 (2011) 841–854

Contents lists available at ScienceDirect

Remote Sensing of Environment

journal homepage: www.elsevier.com/locate/rse

Water property monitoring and assessment for China's inland Lake Taihu from MODIS-Aqua measurements

Menghua Wang [a,*], Wei Shi [a,b], Junwu Tang [c]

[a] NOAA National Environmental Satellite, Data, and Information Service, Center for Satellite Applications and Research, E/RA3, Room 102, 5200 Auth Road, Camp Springs, MD 20746, USA
[b] CIRA at Colorado State University, Fort Collins, Colorado, USA
[c] National Ocean Technology Center, State Oceanic Administration, Tianjin, China

ARTICLE INFO

Article history:
Received 27 August 2010
Received in revised form 17 November 2010
Accepted 18 November 2010
Available online 22 December 2010

Keywords:
Water quality
Remote sensing
Inland freshwater lake

ABSTRACT

We provide results of quantitative measurements and characterization for inland freshwater Lake Taihu from the Moderate Resolution Imaging Spectroradiometer (MODIS) on the satellite Aqua. China's Lake Taihu, which is located in the Yangtze River delta in one of the world's most urbanized and heavily populated areas, contains consistently highly turbid waters in addition to frequent large seasonal algae blooms in various lake regions. Thus, satellite data processing requires use of the shortwave infrared (SWIR) atmospheric correction algorithm. Specifically for Lake Taihu, an iterative SWIR-based atmospheric correction algorithm has been developed and proven to provide reasonably accurate water-leaving radiance spectra data. Using MODIS-Aqua measurements, the blue-green algae bloom in Lake Taihu in 2007 has been studied in detail, demonstrating the importance and usefulness of satellite water color remote sensing for effectively monitoring and managing a bloom event.

Seasonal and interannual variability, as well as spatial distributions, of lake water properties were studied and assessed using the MODIS-Aqua measurements from 2002 to 2008. Results show that overall waters in Lake Taihu are consistently highly turbid all year round, with the winter and summer as the most and least turbid seasons in the lake, respectively. Extremely turbid waters in the winter are primarily attributed to strong winter winds that lead to significant amounts of total suspended sediment (TSS) in the water column. In addition, MODIS-Aqua–measured water-leaving radiance at the blue band is consistently low in various bay regions in Lake Taihu, indicating high algae concentration in these regions. Climatological water property maps, including normalized water-leaving radiance spectra $nL_w(\lambda)$, chlorophyll-a concentration, and water diffuse attenuation coefficient at the wavelength of 490 nm ($K_d(490)$), are derived from all MODIS-Aqua data from 2002 to 2008 for Lake Taihu, showing overall spatial distribution features for the lake water property.

Published by Elsevier Inc.

1. Introduction

China's Lake Taihu, which is located in the Yangtze River delta (Fig. 1) in one of the world's most heavily populated regions with the highest rate of economic development in recent years, provides normal water usage for several million residents in nearby Wuxi City (Fig. 1). Thus, water quality in inland freshwater lakes such as Lake Taihu is vital to human activities and needs and plays a critical role in the regional ecosystem, which may also impact climate changes. Lake Taihu is the third-largest inland freshwater lake in China, with an areal coverage of ~2300 km² and a mean water depth of ~2 m. Lake Taihu's waters are consistently highly turbid, with the exception of East Taihu Bay and some of the East Lake regions (Fig. 1), where waters are often clear, with aquatic vegetation covering the bottom (Ma et al., 2008). In addition, Lake Taihu has frequent algae blooms in the spring-summer, polluting the lake water. The spring 2007 blue-green algae (*Microcystis*) bloom event in Lake Taihu (Guo, 2007; Wang & Shi, 2008) caught the world's attention. Algae-polluted waters in the lake have adversely affected and interrupted the normal life of the several million nearby residents (e.g., Associated Press, 2007). Therefore, there is an urgent need for effectively monitoring and managing water quality in inland freshwater lakes (such as Lake Taihu), and for a broader understanding the optical, biological, and ecological processes and phenomena in all fresh inland waters.

Although in situ measurements can provide details on inland lake water optical, biological, and biogeochemical properties at fixed locations, they have limitations, in particular, the lack of spatial coverage. In addition, long-term in situ measurements in inland lakes are not only labor-intensive, but also often confined to a relatively short period of time, as well as limited and restricted by weather conditions. Satellite remote sensing can provide synoptic views of water properties for the entire lake, with high rates of temporal and spatial coverage. In addition, satellite measurements are highly stable and are necessary for the study and understanding of the lake water optical and bio-optical variations (both short-term and long-term) and their effects on ecosystems. However, satellite ocean (water) color remote sensing has not been routinely used for Lake Taihu (or other turbid lakes) mainly

* Corresponding author.
E-mail address: Menghua.Wang@noaa.gov (M. Wang).

0034-4257/$ – see front matter. Published by Elsevier Inc.
doi:10.1016/j.rse.2010.11.012

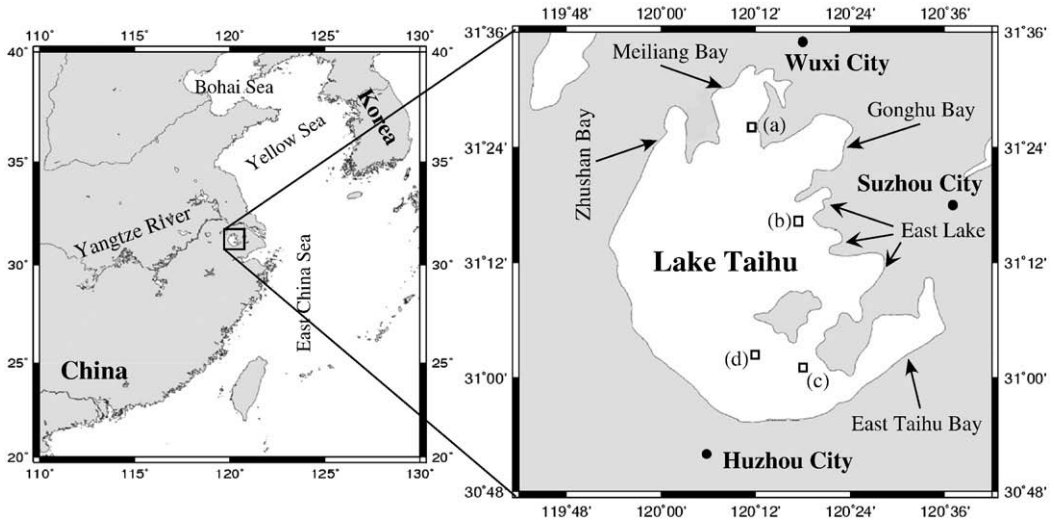

Fig. 1. Maps of China's inland Lake Taihu with indications of four in situ data locations (a)–(d), which correspond to latitudes and longitudes of (31.43°N, 120.20°E), (31.27°N, 120.29°E), (30.95°N, 120.31°E), and (31.06°N, 120.19°E), respectively.

due to difficulty in atmospheric correction for accurately removing atmosphere and water surface effects in deriving normalized water-leaving radiance spectra data (Gordon & Wang, 1994; IOCCG, 2010; Ma et al., 2009). Normalized water-leaving radiance is the radiance that would exit the ocean (in nadir) in the absence of the atmosphere and with the sun at the zenith (Gordon, 1997; Gordon & Wang, 1994; IOCCG, 2010). There are previous studies and applications with various satellite data for Lake Taihu, e.g., (Hu et al., 2010; Jiang et al., 2009; Li et al., 2009; Zhang et al., 2009)), and an overview by Ma et al. (2009) (and references therein). However, quantitative studies to understand and characterize water optical and bio-optical properties in Lake Taihu using extensive satellite ocean color data have not been done. Recently, a shortwave infrared (SWIR) atmospheric correction algorithm was developed and shown to perform well in the coastal turbid waters for deriving ocean color products (Wang, 2007; Wang & Shi, 2005; Wang et al., 2009b). In principle, the SWIR-based algorithm is also applicable for freshwater lake properties from satellite water color measurements.

In this paper, we examine and characterize Lake Taihu water optical and bio-optical properties using measurements from the Moderate Resolution Imaging Spectroradiometer (MODIS) onboard the Aqua satellite platform from 2002 through 2008. The SWIR-based atmospheric correction algorithm with an iterative approach has been developed specifically for Lake Taihu in order to account for some extremely turbid water cases for deriving reasonably accurate normalized water-leaving radiance spectra. Some in situ water optical data in the lake are used for validating MODIS-Aqua derived normalized water-leaving radiance spectra data, showing reasonably good results from satellite measurements. Seasonal and interannual variability of water properties for Lake Taihu is examined; in particular, climatology spatial distributions for various water optical and bio-optical properties in the lake are derived from MODIS-Aqua measurements. In addition, the 2007 blue-green algae bloom event is studied in detail using MODIS-Aqua measurements, demonstrating that satellite water color data can be a useful tool for monitoring and managing lake water quality and can provide better, quicker, and more valuable water information to support improved decisions for local and national management agencies.

2. Satellite-derived water color products for Lake Taihu

2.1. MODIS-Aqua measurements

Since Lake Taihu contains consistently highly turbid waters (Zhang et al., 2006) with significant near-infrared (NIR) water-leaving radiance contributions, the SWIR-based atmospheric correction algorithm (Wang, 2007; Wang & Shi, 2005; Wang et al., 2009b) is required for deriving lake water property data from MODIS measurements. For the NASA standard ocean color data processing, two MODIS NIR bands (748 and 869 nm) have been used for atmospheric correction (Gordon, 1997; Gordon & Wang, 1994) in generating the standard ocean color products. However, the standard MODIS ocean color data processing often fails to produce valid products in highly turbid waters (Wang et al., 2007), e.g., in Lake Taihu, due to incorrect assumptions and/or computation of the NIR water-leaving radiance contributions. It has been demonstrated that the SWIR-based method can produce reasonable MODIS ocean color products along China's east coastal region (Wang et al., 2007), where waters are consistently highly turbid nearly all the time. In addition, the SWIR-based ocean color remote sensing has shown to provide improved satellite-derived water optical and bio-optical parameters in turbid coastal ocean waters (Shi & Wang, 2010, 2010b; Wang et al., 2007), and these data can be used for various applications and studies, e.g., hurricane-driven phytoplankton blooms (Liu et al., 2009; Shi & Wang, 2007a), storm-induced sediment resuspension (Shi & Wang, 2008), storm water plume detection and river plume dynamics (Nezlin et al., 2008; Shi & Wang, 2009a), environmental responses to a land reclamation project in South Korea (Son & Wang, 2009), characterization of regional sediment plumes in the Yellow Sea (Shi & Wang, 2010), and observations of optical and biological property variations in the Korean dump site of the Yellow Sea (Son, et al., 2010), among others.

However, with the SWIR atmospheric correction algorithm using MODIS-Aqua bands 1240 and 2130 nm in deriving water property data for Lake Taihu, we found that the SWIR 1240 nm band is not always black for the entire Lake Taihu, i.e., the water-leaving radiance at 1240 nm is not always negligible for waters in some regions (Shi & Wang, 2009c), in particular, for regions with very significant concentrations of algae (algae blooms), e.g., cases with surface-floating algae (Shi & Wang, 2009b). Therefore, an approach similar to that used for the study of the green macroalgae blooms in the Yellow Sea during the spring-summer of 2008 (Shi & Wang, 2009b) has been developed and implemented in data processing. Specifically, the following data processing procedure has been used for deriving the normalized water-leaving radiance spectra $nL_w(\lambda)$ or the normalized water-leaving reflectance spectra $\rho_{wN}(\lambda)$ (Gordon, 2005; Gordon & Wang, 1994; Morel & Gentili, 1991; Wang, 2006) over Lake Taihu.

(1) First, the SWIR-based atmospheric correction algorithm using MODIS-Aqua SWIR bands of 1240 and 2130 nm is carried out over Lake Taihu, and both water optical property (e.g., $nL_w(\lambda)$)

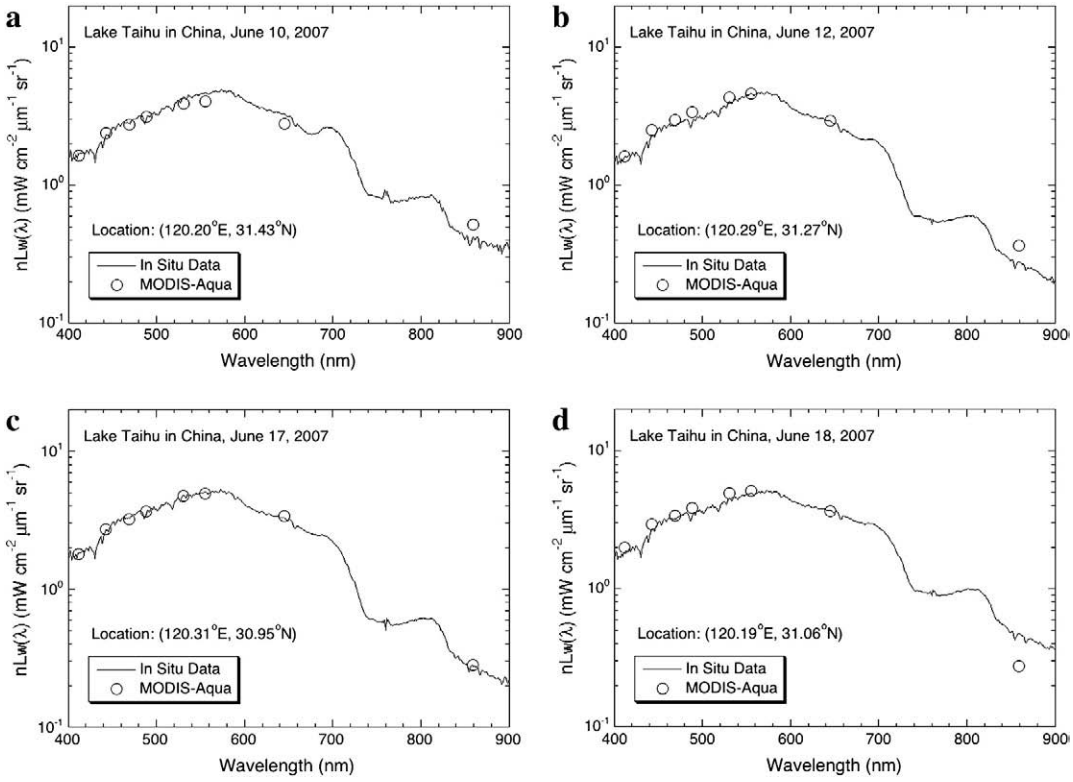

Fig. 2. MODIS-Aqua-derived normalized water-leaving radiance spectra $nL_w(\lambda)$ in Lake Taihu compared with the in situ data that were acquired on (a) June 10, 2007, (b) June 12, 2007, (c) June 17, 2007, and (d) June 18, 2007. The locations in latitude and longitude are indicated in each plot and also shown in Fig. 1.

and aerosol property—in particular, aerosol Ångström exponents, or aerosol models (Wang et al., 2005)—are obtained at the pixel-by-pixel level. The Ångström exponent $\alpha(\lambda)$ is defined as

$$\alpha(\lambda) = log_e\left(\frac{\tau_a(\lambda)}{\tau_a(869)}\right) \Big/ log_e\left(\frac{869}{\lambda}\right)$$

where $\tau_a(\lambda)$ is the aerosol optical thickness at the wavelength λ. Specifically, MODIS-Aqua-derived $\alpha(531)$ value is used. Note that, in the data processing system, each aerosol model has a unique $\alpha(531)$ value (Wang et al., 2005). This is an essential use of the SWIR-based data processing carried out with MODIS SWIR 1240 and 2130 nm bands (Wang, 2007) for Lake Taihu.

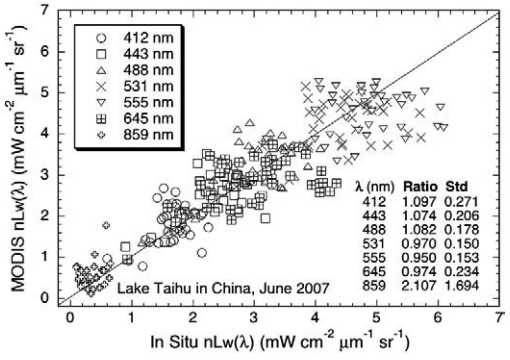

Fig. 3. MODIS-Aqua-derived normalized water-leaving radiance $nL_w(\lambda)$ data in Lake Taihu compared with in situ measurements for wavelengths of 412, 443, 488, 555, 645, and 859 nm. The mean ratio (MODIS-Aqua vs. in situ) and standard deviation (STD) values at each wavelength are listed in the plot and shown in Table 1.

(2) Next, from the derived aerosol Ångström exponent values for each MODIS-Aqua scene, a mean value from a box of 20×20 pixels (~4 km×4 km in the remapped image with ~0.25 km spatial resolution) centered around the central lake region (indicated as "C" in Fig. 4(k)) is derived. In the central lake region, we found that the MODIS SWIR 1240 nm band is generally black (i.e., negligible water-leaving radiance contribution) and can be used for deriving representative aerosol properties for Lake Taihu (e.g., aerosol Ångström exponents or aerosol models).

(3) Finally, using the mean aerosol Ångström exponent derived from step 2, the SWIR atmospheric correction algorithm using a single band at 2130 nm (1240 nm band is not used) can be carried out for the entire lake in deriving the normalized water-leaving radiance spectra $nL_w(\lambda)$ data, as well as other water properties such as chlorophyll-a concentration (Chl-a) (O'Reilly et al., 1998, 2000) and diffuse attenuation coefficient at the wavelength of 490 nm ($K_d(490)$) (Wang et al., 2009a).

It is noted that SWIR-based data processing has been modified to take the input of Ångström exponents for carrying out the single-band atmospheric correction algorithm for deriving water property in Lake Taihu. In the atmospheric correction procedure for retrieval of water

Table 1
Matchup comparison results (Fig. 3) of the $nL_w(\lambda)$ mean ratio (MODIS vs. *in situ*) and the corresponding standard deviation (STD) values for MODIS-Aqua various bands.

Parameter	$nL_w(\lambda)$ Matchup Comparisons						
	412 nm	443 nm	488 nm	531 nm	555 nm	645 nm	859 nm
Mean Ratio†	1.097	1.074	1.082	0.970	0.950	0.974	2.107
STD‡	0.271	0.206	0.178	0.150	0.153	0.234	1.694

† Mean ratio between MODIS vs. *in situ* data.
‡ Standard deviation.

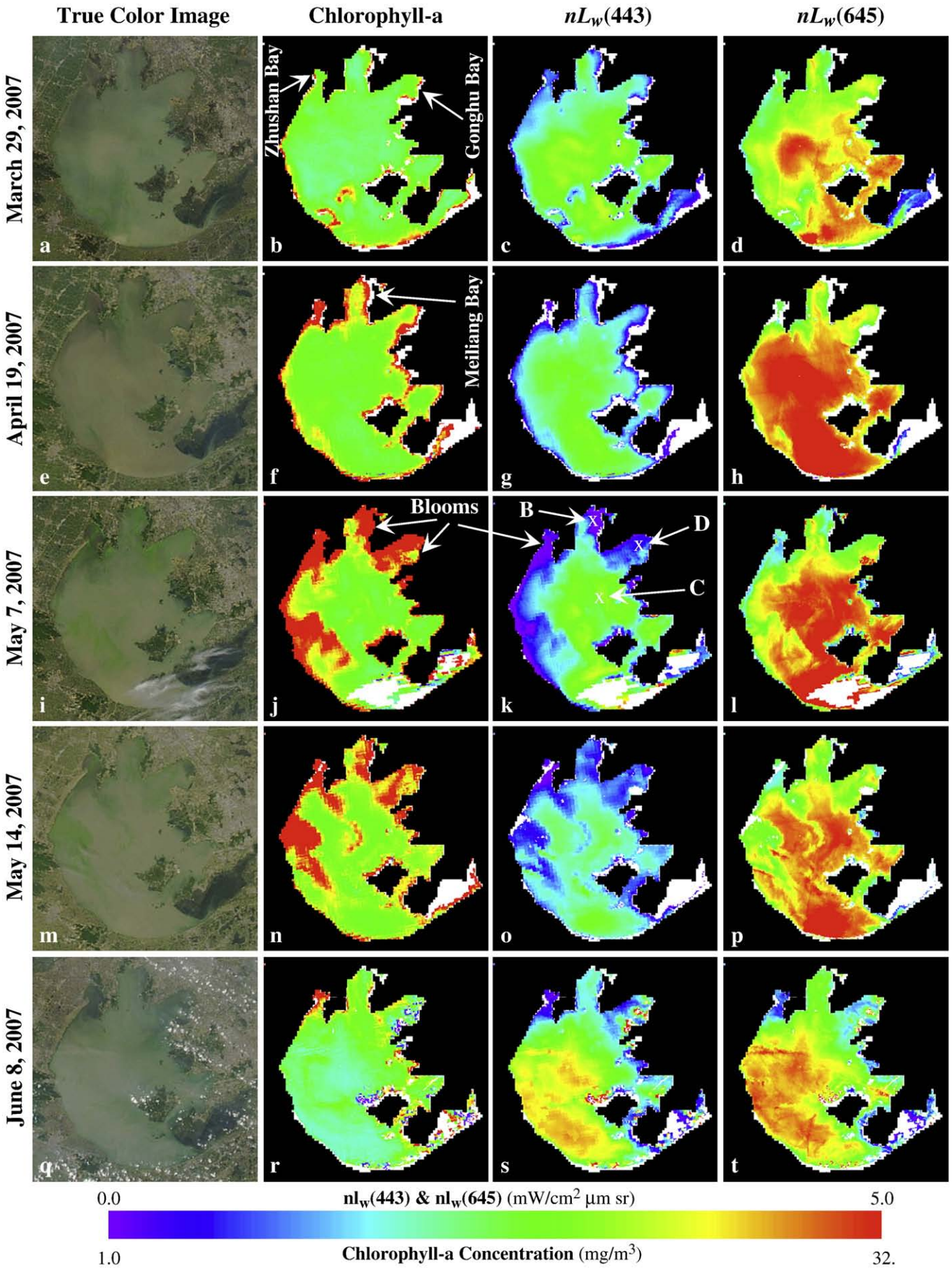

Fig. 4. MODIS-Aqua-measured true color image, Chl-a concentration, $nL_w(443)$, and $nL_w(645)$ (as first to fourth columns) for Lake Taihu on March 29, 2007 (panels a–d), April 19, 2007 (panels e–h), May 7, 2007 (panels i–l), May 14, 2007 (panels m–p), and June 8, 2007 (panels q–t), respectively.

(ocean) color products, appropriate aerosol models are first derived using either sensor-measured two-NIR or two-SWIR radiances (Gordon & Wang, 1994; IOCCG, 2010; Wang, 2007). With the derived aerosol models, aerosol radiance spectra can then be estimated and corrected using the sensor-measured aerosol radiance at the MODIS longer-NIR (i.e., 869 nm) band (Gordon & Wang, 1994) or longer-SWIR (i.e., 2130 nm) band (Wang, 2007). Since each aerosol model corresponds to a unique Ångström exponent value in the data processing system (Wang et al., 2005), using the derived Ångström exponent values (instead of aerosol models) is convenient and efficient for a large volume of data processing, e.g., for MODIS-Aqua multi-year data processing in Lake Taihu.

In summary, the atmospheric correction procedure for Lake Taihu has been carried out iteratively (run twice): first, the most appropriate aerosol Ångström exponent values are derived for each MODIS-Aqua scene over the lake; second, the single-SWIR-band (at 2130 nm) atmospheric correction procedure is carried out using the derived aerosol Ångström exponent values applied to all of Lake Taihu.

2.2. MODIS-Aqua data compared with in situ measurements

During June 10–18, 2007, extensive field campaigns in Lake Taihu were conducted to collect various in situ physical, optical, and biological water data (Jiang et al., 2009). In particular, in situ water-leaving radiance spectra data from 350 to 1050 nm were measured using an Analytical Spectral Devices, Inc. (ASD) FieldSpec Dual UV/VNIR spectrometer, for which the instrument spectral sampling interval is 1.4 nm for its entire spectral coverage (350–1050 nm). The in situ data collection and processing were carried out following the procedures outlined in the NASA ocean optics protocols (Mueller & Fargion, 2002). Specifically, in the in situ data processing, the radiance that is contributed by the water surface reflection from the sky radiance to the instrument detector has been calculated and removed (Tang et al., 2004). Thus, MODIS-Aqua derived normalized water-leaving radiance spectra $nL_w(\lambda)$ in Lake Taihu can be compared with those from in situ measurements. However, due to frequent cloud coverage during the period of field measurements, hardly any satellite data could be matched to contemporaneous in situ measurements. Consequently, MODIS-Aqua $nL_w(\lambda)$ composite imagery for June 2007 has been generated and compared with the in situ data. In fact, for June of 2007 MODIS-Aqua data were collected mainly from June 8 and June 17, 2007. It should be noted that the water optical properties for Lake Taihu are generally relatively stable in summer.

Fig. 2 provides four examples of these validation comparisons. Fig. 2(a)–(d) are $nL_w(\lambda)$ spectra data that were collected at the locations indicated in Fig. 1 marked as (a)–(d), i.e., the corresponding latitudes and longitudes for the data obtained in Fig. 2(a)–(d) are at (31.43°N, 120.20°E) for June 7, 2007, (31.27°N, 120.29°E) for June 12, 2007, (30.95°N, 120.31°E) for June 17, 2007, and (31.06°N, 120.19°E) for June 18, 2007, respectively. MODIS-Aqua-measured $nL_w(\lambda)$ spectra data in Fig. 2 were derived by averaging 5×5 pixels (in the remapped images with ~0.25 km spatial resolution) surrounding the in situ data location. The results in Fig. 2 show that the SWIR-based iterative atmospheric correction algorithm performed reasonably well for these highly turbid inland lake waters. Indeed, both the in situ and MODIS-Aqua data show significantly high NIR water-leaving radiance values, i.e., $nL_w(\lambda)$ values at the wavelength of 859 nm (nL_w(859)) range from ~0.3 to over ~1 mW cm^{-2} μm^{-1} sr^{-1} (see also Fig. 3). For these cases, the MODIS-derived $nL_w(\lambda)$ at the visible bands compare reasonably well with the in situ measurements.

Fig. 3 further shows comparisons between MODIS-Aqua and in situ measured $nL_w(\lambda)$ values at the selected seven MODIS-Aqua bands, including in situ data acquired in Lake Taihu for the time period of June 10–18, 2007, with a total of 40 measurements. Although there are some variations (noise errors) due to both sensor (e.g., poor MODIS SWIR bands performance) and algorithm performance errors (Wang, 2007), as well as some temporal variations in water optical property, results in Fig. 3 show reasonable matchup comparisons between MODIS-Aqua and in situ $nL_w(\lambda)$ measurements. Table 1 provides the mean $nL_w(\lambda)$ ratio values between MODIS-Aqua-derived and in situ measured data for wavelengths of 412, 443, 488, 531, 555, 645, and 859 nm with the corresponding standard deviation (STD) values. It should be noted that the NIR $nL_w(\lambda)$ comparisons show somewhat large differences (also with a large STD value) between satellite and in situ measurements for Lake Taihu, while some previous validation results in China's east coastal region show excellent MODIS-Aqua $nL_w(\lambda)$ data (Wang et al., 2007), particularly for the NIR $nL_w(\lambda)$ data. These large differences in the NIR $nL_w(\lambda)$ data might be due to temporal variations, i.e., resulting from time differences between satellite and in situ measurements. The differences might also be contributed from spatial variations between satellite (5×5 average) and in situ (at one point) measurements.

In summary, validation results show that using the SWIR-based iterative atmospheric correction algorithm for satellite data processing, MODIS-Aqua can produce reasonably good water optical property $nL_w(\lambda)$ data for inland Lake Taihu. MODIS-Aqua derived $nL_w(\lambda)$ spectra data can then be used for retrieval of other water properties for Lake Taihu, e.g., water diffuse attenuation coefficient at the wavelength of 490 nm (K_d(490)) (Lee et al., 2002; Wang et al., 2009a), chlorophyll-a concentration (O'Reilly et al., 1998, 2000) (as an index).

3. Monitoring algae blooms in Lake Taihu

Inland freshwater property data derived from satellite measurements can be useful monitoring and management tools. An example of applications using satellite-derived imageries for inland lake water quality monitoring and management is provided in this section.

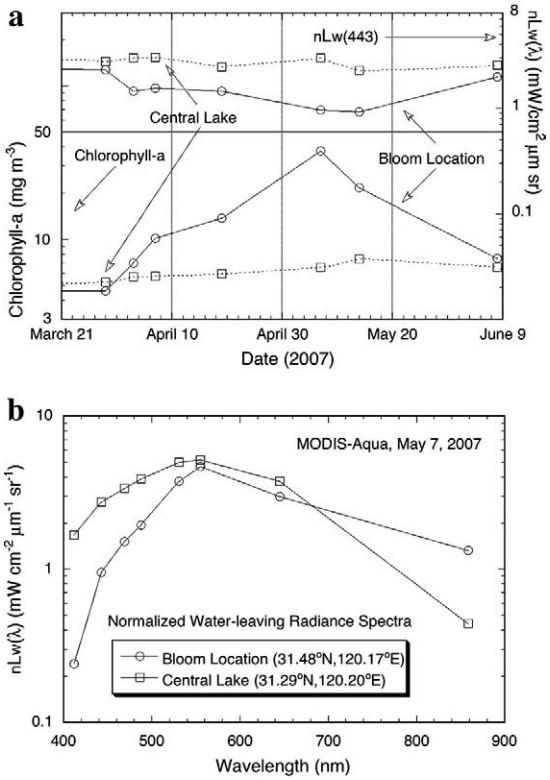

Fig. 5. MODIS-Aqua-derived (a) time series (March 29 to June 8, 2007) for chlorophyll-a (bottom portion and scale at left) and $nL_w(443)$ (top portion and scale at right) and (b) $nL_w(\lambda)$ spectra on May 7, 2007 for the algae bloom contaminated (location indicated as "B" in Fig. 4(k)) and non-contaminated (location indicated as "C" in Fig. 4(k)) waters in Lake Taihu.

3.1. 2007 blue-green algae bloom

During the spring of 2007, a massive blue-green algae (*Microcystis*) bloom broke out in Lake Taihu (Guo, 2007). The algae blooms produced foul odors and toxic compounds, making the water unusable. This massive bloom event led to an environmental crisis that cut off the tap water supply to several million residents in nearby Wuxi City (Fig. 1) in the Jiangsu Province, and negatively impacted human activities and needs (Associated Press, 2007). The 2007 bloom event caught the local government and residents of Wuxi City by surprise, forcing unprepared residents to rush to buy bottled water for their normal usage. As such, the outbreak was identified as a major natural disaster by the Chinese government.

3.2. Satellite observations and monitoring

During the 2007 bloom event, MODIS-Aqua acquired several clear-sky images from March 29 to June 8, 2007, capturing some important stages of the moments as the bloom evolved and developed (Wang & Shi, 2008). Figs. 4 and 5 provide examples of MODIS-Aqua derived water optical and biological properties during the entire bloom event. MODIS-observed imagery of Chl-a concentration (O'Reilly et al., 1998, 2000), i.e., Fig. 4(b), (f), (j), (n), and (r), and $nL_w(\lambda)$ at 443 nm (nL_w(443)), i.e., Fig. 4(c), (g), (k), (o), and (s), and 645 nm (nL_w(645)), i.e., Fig. 4(d), (h), (l), (p), and (t), show the spatial variation of the lake's optical and biological properties in various stages of the blue-green algae bloom. The MODIS-Aqua corresponding true color images are shown in Fig. 4(a), (e), (i), (m), and (q) with the spatial resolution of ~0.25 km. These images represent satellite-measured water property at various stages in the bloom development: before the bloom started on March 29, 2007 (Fig. 4(a)–(d)), beginning of the bloom on April 9, 2007 (Fig. 4(e)–(h)), during the peak of the blue-green algae bloom event on May 7, 2007 (Fig. 4(i)–(l)), when the algae bloom started to die down on May 14, 2007 (Fig. 4(m)–(p)), and after the bloom event on June 8, 2007 (Fig. 4(q)–(t)).

It should be noted that for the complex turbid waters such as in Lake Taihu, a good deal of uncertainty lies in the current satellite bio-optical algorithm (O'Reilly et al., 1998, 2000) in deriving chlorophyll-a values, and may require new approaches (Gitelson et al., 2007). Thus, we use chlorophyll-a as an index (qualitatively) for bloom indication (i.e., high Chl-a values). Also, we found that (Shi & Wang, 2007b) for these cases, aerosols presented in the region were not strongly absorbing. For waters with and without contamination by the algae bloom in Lake Taihu (locations indicated in Fig. 4(k) as "B" and "C"), Fig. 5(a) provides the temporal variation (March 29 to June 8, 2007) for Chl-a (bottom panel) and nL_w(443) (top panel) derived from

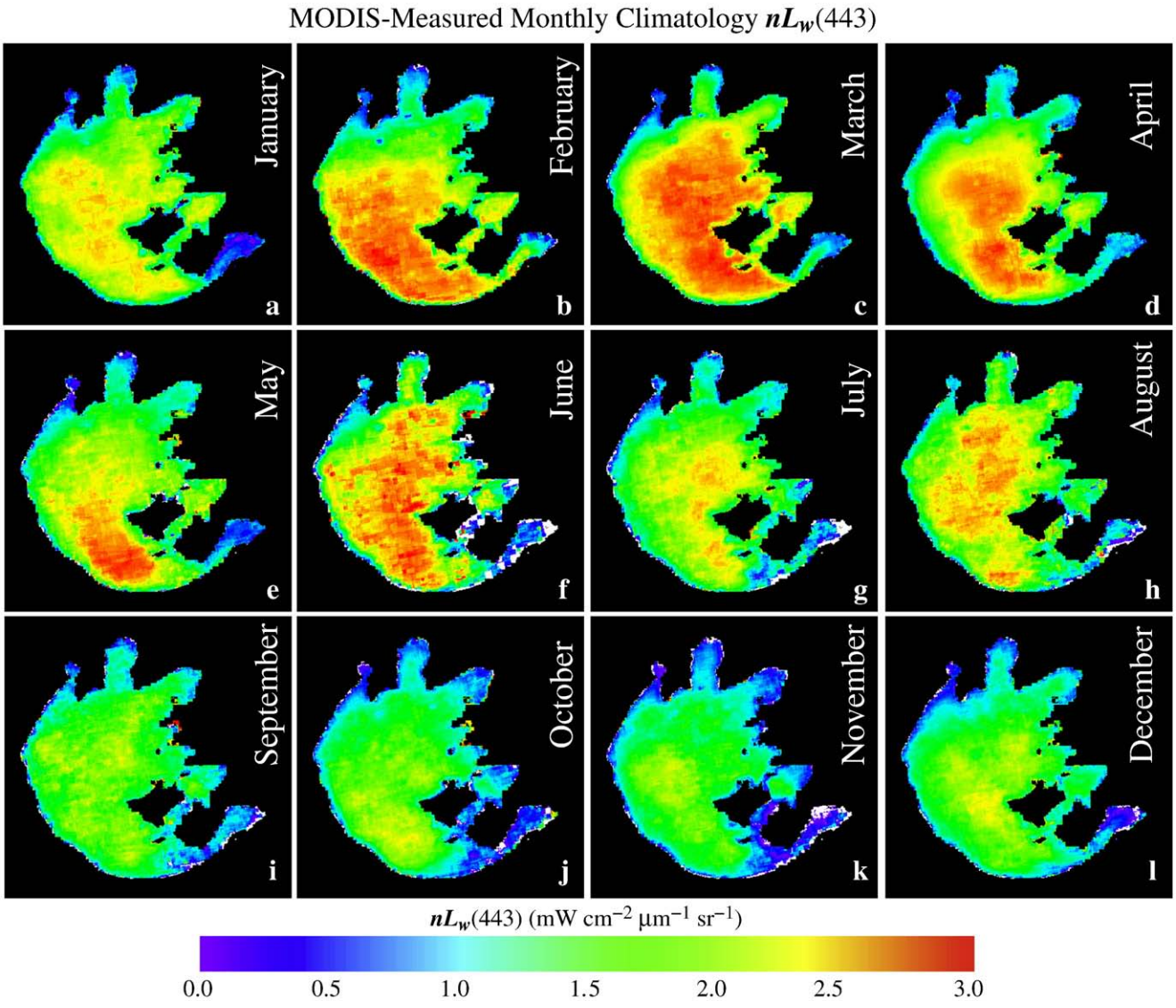

Fig. 6. MODIS-Aqua-measured (2002–2008) monthly climatology nL_w(443) in Lake Taihu from January to December as shown in panels (a)–(l).

MODIS-Aqua measurements for the entire bloom event. Fig. 5(b) compares the $nL_w(\lambda)$ spectra data for waters with and without contamination by the blue-green algae bloom in Lake Taihu (locations as "B" and "C" in Fig. 4(k)).

MODIS-Aqua Chl-a and $nL_w(443)$ data (Figs. 4 and 5(a)) show that the blue-green algae bloom contamination in Meiliang Bay started in the first week of April, peaked around May 7, with the event ending in the beginning of June. Meiliang Bay in Lake Taihu is one of main water supply sources for nearby Wuxi City and one of the regions where waters were considerably contaminated by the blue-green algae bloom. In fact, in waters adjacent to Wuxi City at a location of (31.53°N, 120.19°E), the MODIS-Aqua-derived Chl-a concentrations (used as an index) peaked to ~181 and ~127 mg/m^3 on May 7 and May 14, respectively. The major blue-green algae blooms mainly occurred in Meiliang Bay, Gonghu Bay, and Zhushan Bay, as well as the west region of Lake Taihu (Fig. 4). During the event, chlorophyll-a values for the uncontaminated waters, e.g., in central lake regions, had a relatively low value (bottom panel in Fig. 5(a)). Results in Figs. 4 and 5(a) show that this algae bloom, with its dramatically elevated pigment concentrations, resulted in a significant drop of the MODIS-derived normalized water-leaving radiance at the blue band (443 nm) because of the strong algae absorption at that wavelength (Gordon & Morel, 1983; Roesler & Perry, 1995; Roesler et al., 1989).

Fig. 4 also provides results of normalized water-leaving radiance at the wavelength of 645 nm ($nL_w(645)$), which can be used to relate the water near-surface total suspended sediment (TSS) concentration (Miller & McKee, 2004; Shi & Wang, 2009a), for the entire bloom event in Lake Taihu. There were significant changes of $nL_w(645)$ in Lake Taihu for the bloom period, with considerable highs in its elevated values and coverage on April 19, 2007 (Fig. 4(h)). In fact, $nL_w(645)$ values at the bloom-contaminated regions, e.g., Meiliang Bay, Gonghu Bay, and Zhushan Bay, were relatively stable during the bloom event, while the central lake region had a significant $nL_w(645)$ variation in the period. As expected, $nL_w(\lambda)$ spectra data show significant different radiance distributions for the region with and without algae contamination (Fig. 5(b)). In particular, for the bloom-contaminated waters, $nL_w(\lambda)$ data at blue wavelengths are remarkably lower than those from non-contaminated waters due to the strong algae absorption (Roesler & Perry, 1995), while at the green band (e.g., 555 nm) $nL_w(\lambda)$ values from two regions are more or less similar (Fig. 5(b)).

4. Characterization of water optical properties for Lake Taihu

MODIS-Aqua measurements from 2002 to 2008 in Lake Taihu were acquired to produce water property data using the SWIR-based iterative atmospheric correction algorithm. These satellite remote sensing data

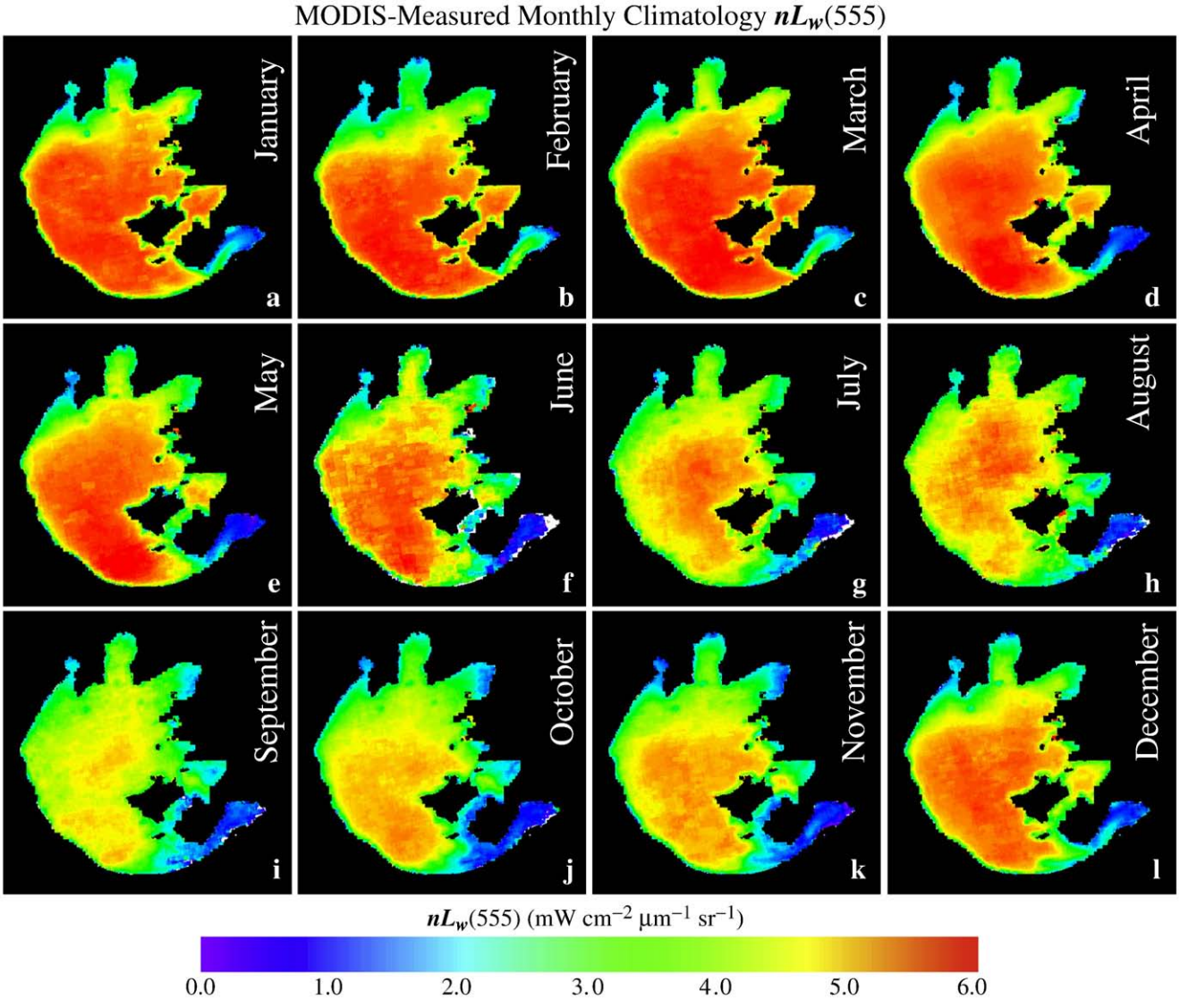

Fig. 7. MODIS-Aqua-measured (2002–2008) monthly climatology $nL_w(555)$ in Lake Taihu from January to December as shown in panels (a)–(l).

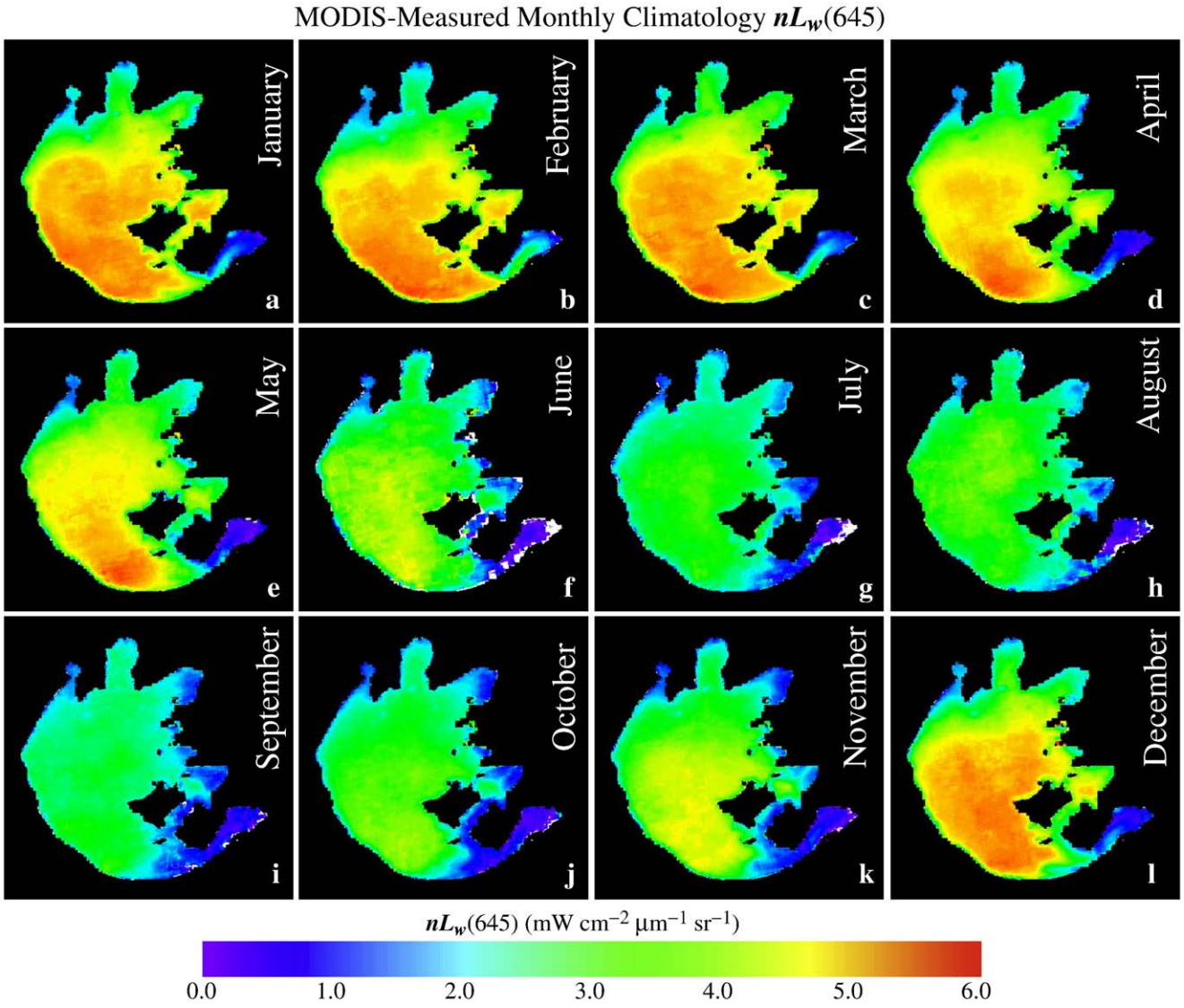

Fig. 8. MODIS-Aqua-measured (2002–2008) monthly climatology $nL_w(645)$ in Lake Taihu from January to December as shown in panels (a)–(l).

are used for characterizing water optical properties and water quality for Lake Taihu. Detailed results and discussions are provided in the following sections.

4.1. Seasonal and spatial variations of MODIS $nL_w(\lambda)$ spectra data

Figs. 6–9 provide monthly climatology $nL_w(\lambda)$ images at wavelengths of 443, 555, 645, and 859 nm, respectively, for the entire lake. These $nL_w(\lambda)$ images were derived from MODIS-Aqua measurements from 2002 to 2008 using the SWIR-based atmospheric correction algorithm (Wang, 2007; Wang et al., 2009b) and modified with an iterative approach. Thus, $nL_w(\lambda)$ results in Figs. 6–9 provide overall characteristics of normalized water-leaving radiance distributions both spatially and temporally for Lake Taihu. It is noted that color scales in Figs. 6–9 are different.

Fig. 6(a)–(l) shows monthly climatology (January to December) of $nL_w(\lambda)$ at the wavelength of 443 nm ($nL_w(443)$), representing characterization of algae absorption distributions for Lake Taihu. Spatially, low $nL_w(443)$ values are observed in various bay regions, e.g., the Meiliang Bay, Gonghu Bay, and Zhushan Bay, compared with other lake regions, particularly in the central lake region. Overall, for most of the lake, high $nL_w(443)$ values are in the spring season, while lows are shown in the fall season. On the other hand, monthly climatology $nL_w(555)$ images (Fig. 7) show relatively stable values throughout the year for Meiliang Bay, Gonghu Bay, and Zhushan Bay, while there are significant seasonal changes in $nL_w(555)$ for most of the other lake regions. For most of the lake regions, high $nL_w(555)$ values are observed in the winter-spring seasons and low values are shown in the summer-fall seasons. These $nL_w(555)$ variations are mainly influenced by changes of the TSS concentration in the lake. The TSS spatial and seasonal variations in Lake Taihu are also represented through monthly climatology results in $nL_w(645)$ (Fig. 8) that can be related to TSS concentration (Miller & McKee, 2004; Shi & Wang, 2009a; Zhang et al., 2010), with highs in the winter–spring seasons (December to May) and lows in the summer-fall seasons (June to November).

Furthermore, results of the NIR water-leaving radiance contributions $nL_w(859)$ for Lake Taihu are provided in Fig. 9. As expected, the seasonal pattern of $nL_w(859)$ is similar to that of $nL_w(645)$, with highs in the winter-spring and lows in the summer–fall seasons for most of the lake regions. Clearly, $nL_w(859)$ variation in Lake Taihu is also mainly controlled and influenced by the TSS variation in the lake. However, results in Fig. 9 show some high $nL_w(859)$ values during the spring in various bay regions, e.g., Meiliang Bay in May (Fig. 9(e)), due to algae blooms. High concentrations of algae lead to large NIR $nL_w(\lambda)$ contributions (Siegel et al., 2000). Fig. 9 shows that December is the month for the most turbid water for Lake Taihu with the largest nL_w

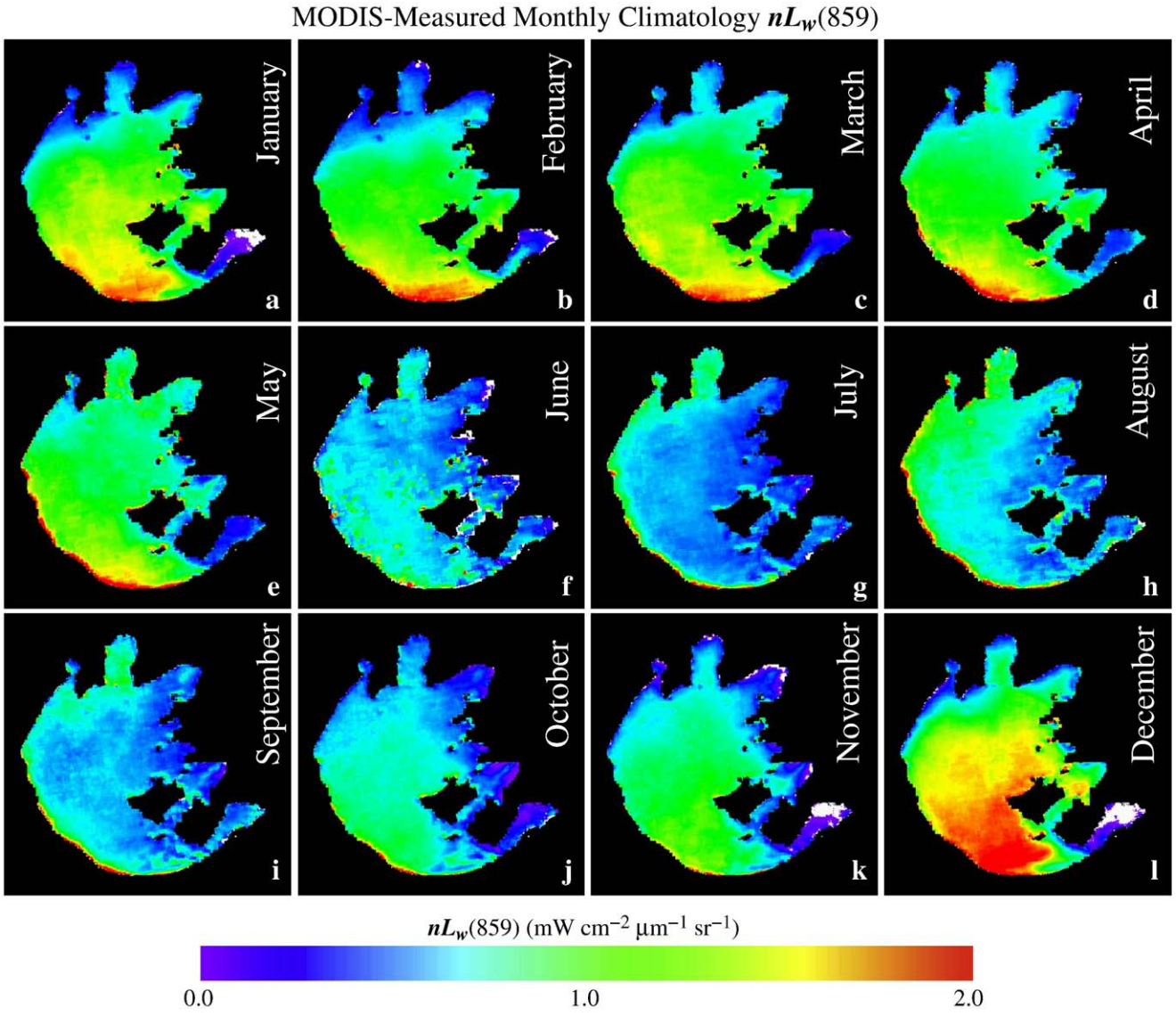

Fig. 9. MODIS-Aqua-measured (2002–2008) monthly climatology $nL_w(859)$ in Lake Taihu from January to December as shown in panels (a)–(l).

(859) located in the lower western part of the lake (Fig. 9(l)). It is important to note that for Lake Taihu $nL_w(859)$ contribution is significant over most of the lake and has to be accurately accounted for in satellite remote sensing of the lake water property with the NIR atmospheric correction algorithm.

It should also be noted that for the East Taihu Bay region (Fig. 1), the water optical properties in Figs. 6–9 clearly show more or less typical clear water characteristics, different from other Lake Taihu regions. However, with such shallow and clear waters in East Taihu Bay (Ma et al., 2008), the bottom radiance contributions are also likely included in the MODIS-derived $nL_w(\lambda)$ for the region, in particular, for the visible bands where water absorption is low (Hale & Querry, 1973). In fact, the bottom radiance contributions in the region may be useful to monitor and understand the aquatic vegetation variations.

4.2. Seasonal and spatial variations of water clarity in Lake Taihu

Water clarity in Lake Taihu can be characterized using the water diffuse attenuation coefficient at the wavelength of 490 nm, $K_d(490)$, which can be derived using a newly developed satellite $K_d(490)$ algorithm for turbid waters (Wang et al., 2009a). Waters with high $K_d(490)$ values represent less water clarity (more turbid), and high-clarity waters have low $K_d(490)$ values. The new $K_d(490)$ model (Wang et al., 2009a) combines the current empirical (or semi-analytical) algorithm for open oceans (Lee et al., 2002; Morel et al., 2007; Mueller, 2000) and a newly-developed semi-analytical $K_d(490)$ model for turbid coastal waters, which is based on the fact that the backscattering coefficient at the wavelength of 490 nm can be accurately correlated to the reflectance at red bands for the turbid waters (Wang et al., 2009a). Some validation results show that the new $K_d(490)$ model can accurately estimate diffuse attenuation coefficient $K_d(490)$ for both clear and turbid waters, e.g., with a mean ratio value (MODIS-derived vs. in situ data) of 1.037 (Wang et al., 2009a). Particularly, compared with the in situ measurements, the new $K_d(490)$ algorithm shows considerably improved accuracy over coastal turbid waters, i.e., waters with high $K_d(490)$ values.

Fig. 10 provides monthly climatology images of the MODIS-Aqua derived $K_d(490)$ in Lake Taihu using the SWIR-based iterative atmospheric correction algorithm (Wang, 2007) and a new $K_d(490)$ method (Wang et al., 2009a). Overall, Lake Taihu waters are more turbid (less clarity) in the winter-spring seasons than the summer-fall seasons. In fact, peak $K_d(490)$ values appear around December, and the lowest value is around September. The spatial distribution of $K_d(490)$ is quite similar to those of $nL_w(645)$ and $nL_w(859)$ images, with highs at the lower western regions of Lake Taihu (e.g., Fig. 10(l)). Again, $K_d(490)$ values in the East Taihu Bay region are consistently low as for typical clear waters.

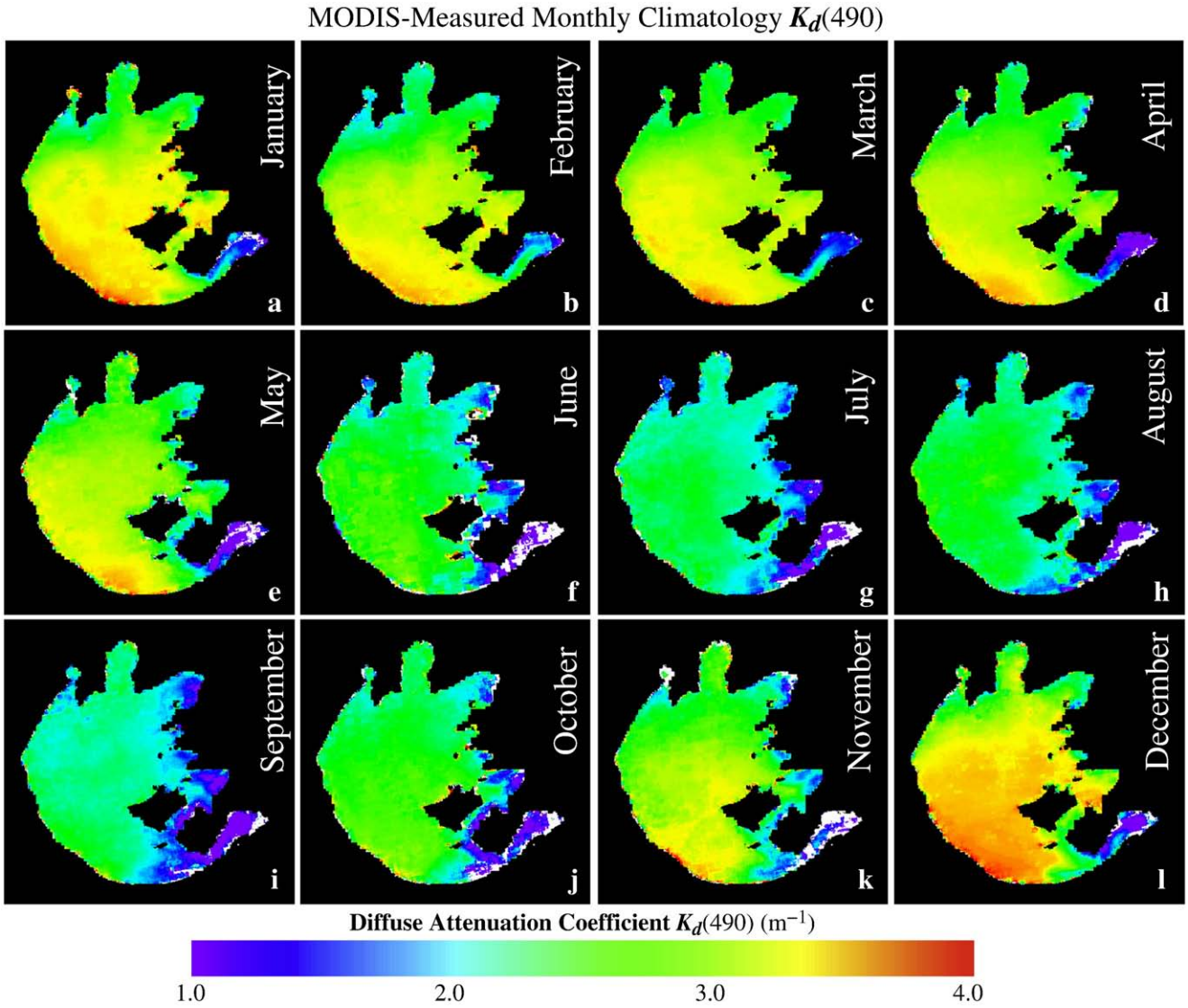

Fig. 10. MODIS-Aqua-measured (2002–2008) monthly climatology K_d(490) in Lake Taihu from January to December as shown in panels (a)–(l).

4.3. Quantitative assessments of water property

Some detailed quantitative assessments and characterizations of water property for Lake Taihu are provided in Figs. 11–13. Fig. 11 shows the seasonal climatology normalized water-leaving reflectance spectra (Wang, 1999), $\rho_{wN}(\lambda)$, for various regions in Lake Taihu for the months of January, April, July, and October, respectively, representing four seasons. Fig. 11(a)–(d) are mean $\rho_{wN}(\lambda)$ spectra data as a function of the wavelength for four months (January, April, July, and October) from the entire Lake Taihu, central region of the lake (location indicated as "C" in Fig. 4(k)), Meiliang Bay (location indicated as "B" in Fig. 4(k)), and Gonghu Bay (location indicated as "D" in Fig. 4(k)), respectively. Overall, Lake Taihu shows typical characteristics of highly turbid (sediment-dominated) waters with $\rho_{wN}(\lambda)$ peaks at green-red wavelengths (Fig. 11(a)). In particular, considerable elevations of $\rho_{wN}(\lambda)$ at red-NIR wavelengths are observed during the winter-spring seasons, showing significantly enhanced water turbidity in these seasons. In fact, during the summer-fall seasons, $\rho_{wN}(\lambda)$ peaks at the green band (Fig. 11(a)). Results from central Lake Taihu in Fig. 11(b) are similar to those from the entire lake (Fig. 11(a)). The reflectance $\rho_{wN}(\lambda)$ spectra variations are primarily influenced by the TSS concentration in the water column, i.e., high TSS values lead to the $\rho_{wN}(\lambda)$ spectra peak shifted from the green to red band with significantly increased NIR $\rho_{wN}(\lambda)$ contributions (e.g., Fig. 11(a) and (b)). On the other hand, $\rho_{wN}(\lambda)$ results in Meiliang Bay (Fig. 11(c)) and Gonghu Bay (Fig. 11(d)) show consistently low $\rho_{wN}(\lambda)$ values in the blue bands, resulting from the algae absorption. Particularly, in Meiliang Bay, there is much less seasonal variation in $\rho_{wN}(\lambda)$ spectra (Fig. 11(c)). In addition, for the both bays during the spring, while $\rho_{wN}(\lambda)$ values in the blue bands are low, the NIR $\rho_{wN}(\lambda)$ values increased, representing enhanced NIR $\rho_{wN}(\lambda)$ contributions from increased algae in the region. Results of the water optical variation in Lake Taihu (Fig. 11) are consistent with results discussed previously.

Fig. 12 further shows temporal (interannual) variations of MODIS-Aqua derived $nL_w(\lambda)$ at wavelengths 443, 555, 645, and 859 nm for various regions in Lake Taihu (i.e., the central lake, Gonghu Bay, and Meiliang Bay). Although interannual repeatability is quite good for $nL_w(\lambda)$ in various regions in Lake Taihu, some regional differences are presented. $nL_w(\lambda)$ at the wavelength of 443 nm (Fig. 12(a)) shows peaks at early spring and late summer, but also has some obvious lows (troughs) during late spring to early summer since 2005, indicating more blooms in recent years for the region (Hu et al., 2010). The lowest $nL_w(\lambda)$ value at the blue band usually appears in early winter (December). On the other hand, $nL_w(\lambda)$ at the wavelength of 555 nm (Fig. 12(b)) presents consistent peaks during the spring for Meiliang

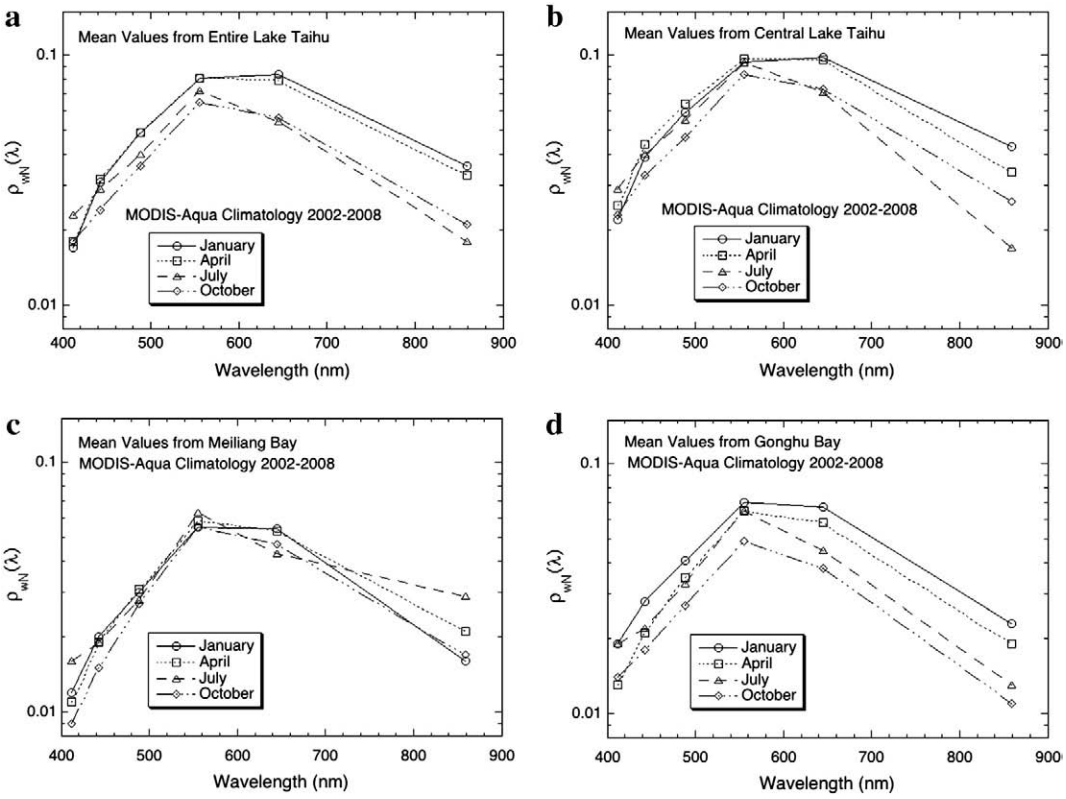

Fig. 11. MODIS-Aqua-measured monthly climatology normalized water-leaving reflectance spectra $\rho_{wN}(\lambda)$ for months of January, April, July, and October, and for the region of (a) entire Lake Taihu, (b) central Lake Taihu, (c) Meiliang Bay, and (d) Gonghu Bay, respectively.

Bay, while other regions have different optical features. In particular, for 2007 when huge blue-green algae blooms happened, $nL_w(555)$ shows a peak value during spring-summer in Meiliang Bay, while in the central lake region $nL_w(555)$ has a opposite lowest value. The red band $nL_w(\lambda)$ value, which can be related to TSS concentration, generally peaks in winter and has lows in late summer (Fig. 12(c)).

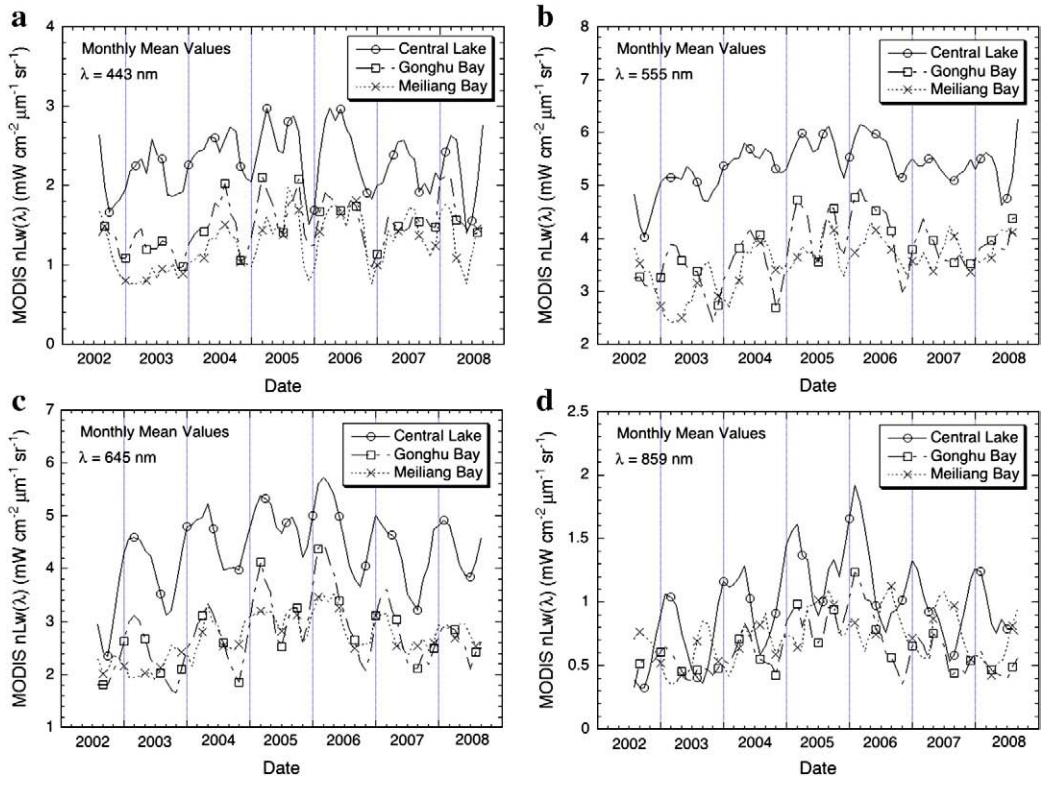

Fig. 12. MODIS-Aqua-measured time series of normalized water-leaving radiance $nL_w(\lambda)$ at the wavelength of (a) 443 nm, (b) 555 nm, (c) 645 nm, and (d) 859 nm for the regions of central lake, Gonghu Bay, and Meiliang Bay in Lake Taihu.

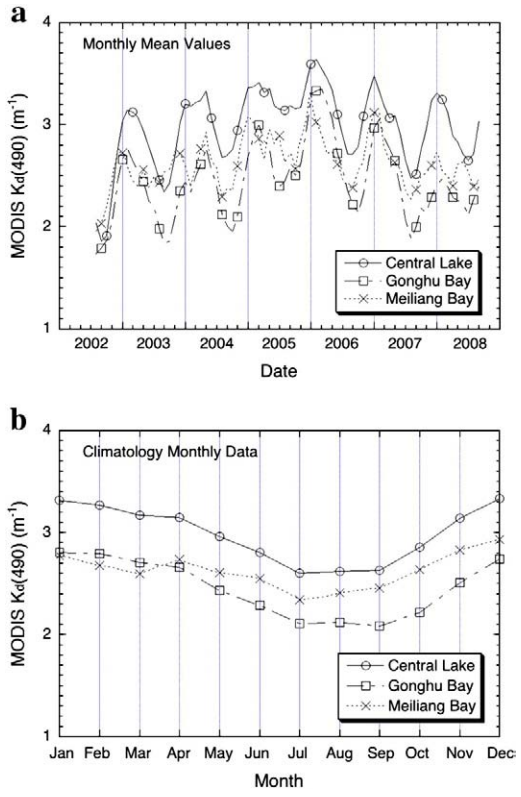

Fig. 13. MODIS-Aqua-measured water diffuse attenuation coefficient at the wavelength of 490 nm (K_d(490)) for the lake regions of the central lake, Gonghu Bay, and Meiliang Bay, respectively, represented as (a) time series (interannual variability) and (b) seasonal variability.

The highs and lows in nL_w(645) are very consistently presented in all three regions, although significantly high values are in the central lake region (i.e., high TSS values).

Some interesting characteristics are shown in the NIR $nL_w(\lambda)$ variations for three regions in Lake Taihu (Fig. 12(d)). In fact, these three regions have different nL_w(859) distributions; in particular, the central lake region and Meiliang Bay have opposite highs/lows in nL_w(859) variations. For the central lake region, peaks and troughs appear in winter and summer, respectively, while for Meiliang Bay highs and lows are in early summer and winter instead (Fig. 12(d)). The primary mechanisms for significant nL_w(859) contributions and variations are different: the central lake water is dominated by the variation of TSS concentration, while the change of the algae concentration is a main factor for high nL_w(859) contributions in Meiliang Bay. It should be noted that, in general, Lake Taihu has significantly high NIR $nL_w(\lambda)$ contributions, in particular, in the lower western part of lake region.

Seasonal and interannual variations of water diffuse attenuation coefficient at the wavelength of 490 nm, K_d(490), for the selected three regions (central lake, Gonghu Bay, and Meiliang Bay) are provided in Fig. 13. As discussed in previous sections, K_d(490) can be used as a measure for the water clarity. Consistent with $nL_w(\lambda)$ results, waters in Lake Taihu are extremely turbid in the winter with K_d(490) values reaching ~3.3 m^{-1} for the central lake region. The seasonally lowest K_d(490) value for the central lake region is ~2.6 m^{-1} (Fig. 13), still highly turbid (Shi & Wang, 2010b). It is interesting to note that, for Meiliang Bay, seasonal K_d(490) value has a peak in April (Fig. 13(b)), representing algae effects on the water clarity in the region. Quantitatively, for the central lake (representing most of Lake Taihu), Gonghu Bay, and Meiliang Bay, K_d(490) values vary from ~2.6 to ~3.3 m^{-1}, ~2.1 to ~2.8 m^{-1}, and ~2.3 to ~3.0 m^{-1}, respectively.

5. Satellite-derived climatology water property maps for Lake Taihu

Using MODIS-Aqua for all measurements from 2002 to 2008 in Lake Taihu, climatology maps for various water properties were generated and are presented in Fig. 14. Fig. 14(a)–(f) provide Lake Taihu's climatology maps of nL_w(443), nL_w(555), nL_w(645), nL_w(859), Chl-a, and K_d(490), respectively. Again, the Chl-a map (Fig. 14(e)) is as an index for showing locations with the high algae concentration.

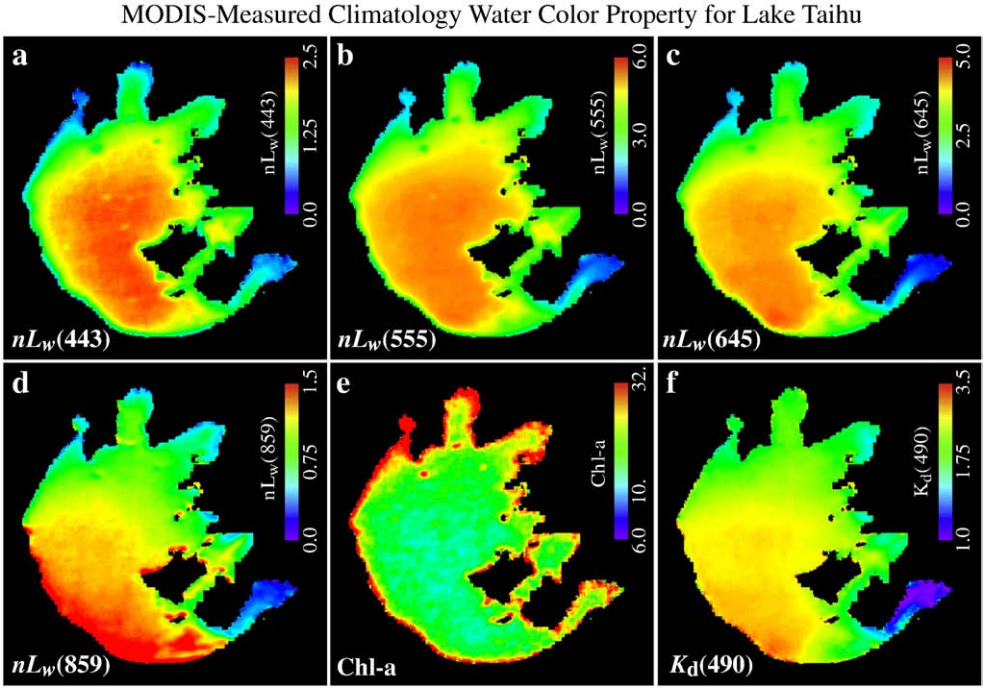

Fig. 14. MODIS-Aqua-derived various climatology water property maps of Lake Taihu for parameters of (a) nL_w(443), (b) nL_w(555), (c) nL_w(645), (d) nL_w(859), (e) Chl-a (in log-scale), and (f) K_d(490), respectively. Note that nL_w(443), nL_w(555), nL_w(645), and nL_w(859) are all in mW cm^{-2} μm^{-1} sr^{-1}, Chl-a is in mg m^{-3}, and K_d(490) is in m^{-1}.

Climatology maps in Fig. 14 have clearly shown overall spatial distribution of water properties for Lake Taihu. Across the radiance spectrum from the blue to NIR, high $nL_w(\lambda)$ contributions are found in most of the central lake regions (Fig. 14(a)–(d)), while high chlorophyll-a values (algae concentrations) are consistently presented in Meiliang Bay, Gonghu Bay, and Zhushan Bay (Fig. 14(e)). Overall, Lake Taihu is generally highly turbid, in particular, for regions in the lower parts of the lake (Fig. 14(f)). In fact, water turbidity can also be seen from the NIR $nL_w(\lambda)$ climatology map in Fig. 14(d), showing a similar pattern and spatial distribution in $nL_w(859)$ as from $K_d(490)$ map in Fig. 14(f). In addition, results in Fig. 14(d) clearly show that the NIR water-leaving radiance contributions in Lake Taihu are indeed very significant and need to be accurately accounted for in order to derive accurate water property data from satellite measurements using the NIR algorithm (Gordon & Wang, 1994). Without account for the NIR $nL_w(\lambda)$ contributions, the standard (NIR) atmospheric correction algorithm will certainly fail in Lake Taihu with such extremely turbid waters.

6. Discussions and conclusion

With MODIS-Aqua measurements from 2002 to 2008, water properties of Lake Taihu in China have been studied and characterized using the SWIR-based atmospheric correction algorithm for the data processing. This is the first time that ocean color satellite measurements have been used extensively to quantitatively study and understand water optical and bio-optical properties for a highly turbid inland freshwater lake. For this highly turbid lake with frequent seasonal algae blooms in various bay regions, the SWIR-based atmospheric correction algorithm has been further modified to use an iterative approach to account for non-negligible lake water contributions at the MODIS-Aqua 1240 nm band. Some validation results, comparing MODIS-Aqua-derived $nL_w(\lambda)$ with those from in situ measurements, show that with the SWIR-based iterative approach MODIS-Aqua can produce reasonably good water optical property $nL_w(\lambda)$ data for the lake. Thus, MODIS-Aqua measurements have been used to quantify the seasonal and interannual variability of water optical and bio-optical properties for Lake Taihu.

Overall, waters in Lake Taihu are consistently highly turbid all year-round, and the highest and lowest $K_d(490)$ values are usually in winter and summer, respectively. MODIS-Aqua-measured $nL_w(\lambda)$ at the blue band ($nL_w(443)$) is consistently low in various bay regions, e.g., Meiliang Bay, Gonghu Bay, and Zhushan Bay, representing high algae absorption for these bay regions in Lake Taihu. Particularly, for these bay regions low $nL_w(443)$ values are often observed during late spring to early summer, especially in recent years. Similar results from MODIS-Aqua-derived chlorophyll-a concentration (as an index) are shown in the lake, with high Chl-a values usually appearing in the bay regions. These results are consistent with field observations of seasonal algae blooms in the lake, e.g., the large blue-green algae blooms in late spring of 2007. On the other hand, the $nL_w(645)$ value, which can be related to the TSS concentration in the water column, shows highs and lows in the winter and summer for Lake Taihu, respectively. The peak value in $nL_w(645)$ (or TSS value) is mainly due to high winter winds that lead to increased TSS value in the region (Ding, 1994). Spatially, consistently high $nL_w(645)$ values are primarily in the lower part of the lake, while low values are shown in various bay regions. The seasonal and spatial distributions of the NIR water-leaving radiance $nL_w(859)$ for the lake are similar to those of $nL_w(645)$. Importantly, $nL_w(859)$ values are usually significantly high for the entire lake; in particular, the peak values of $nL_w(859)$ are in the lower part of the lake. Thus, for the satellite remote sensing of the lake water properties, the satellite data processing needs to account for the NIR water radiance contributions. It is noted that accurately estimation of Chl-a values in Lake Taihu from satellite measurements may require regional algorithms and/or new approaches.

This study has also demonstrated an important application for monitoring inland freshwater optical and biological properties, as well as water quality, using the satellite water (ocean) color measurements. In particular, satellite remote sensing data can be used synoptically for monitoring and quantifying algae blooms in the inland freshwater lake, providing useful monitoring and management tools for understanding optical, biological, and ecological processes and phenomena in inland lake waters, responsive to needs identified in a 2007 Global Earth Observing System of Systems (GEOSS) workshop on remote sensing of water quality (http://www.earthobservations.org/geoss_wa.shtml). Indeed, the satellite-derived imagery can be a significant contribution to an algae bloom warning system that will provide useful information for local governments to monitor and prepare for such events in advance.

Acknowledgments

This research was supported by NASA and NOAA funding and grants. The MODIS L1B data were obtained from the NASA/GSFC MODAPS Services website. We thank four anonymous reviewers for their constructive comments that improved the manuscript. The views, opinions, and findings contained in this paper are those of the authors and should not be construed as an official NOAA or U.S. Government position, policy, or decision.

References

Associated Press (2007). Algae smother Chinese lake, millions panic. MSNBC. May 31, 2007. http://www.msnbc.msn.com/id/18959222/from/RS.1

Ding, Y. H. (1994). *Monsoons over China.*: Kluwer Academic Publishers. 419 pp.

Gitelson, A. A., Schalles, J. F., & Hladik, C. M. (2007). Remote chlorophyll-a retrieval in turbid, productive estuaries: Chesapeake Bay case study. *Remote Sensing of Environment*, *109*, 464−472. doi:10.1016/j.rse.2007.01.016

Gordon, H. R. (1997). Atmospheric correction of ocean color imagery in the Earth Observing System era. *Journal of Geophysical Research*, *102*, 17,081−17,106.

Gordon, H. R. (2005). Normalized water-leaving radiance: Revisiting the influence of surface roughness. *Applied Optics*, *44*, 241−248.

Gordon, H. R., & Morel, A. (1983). *Remote assessment of ocean color for interpretation of satellite visible imagery: A review.*New York: Springer-Verlag. 114 pp.

Gordon, H. R., & Wang, M. (1994). Retrieval of water-leaving radiance and aerosol optical thickness over the oceans with SeaWiFS: A preliminary algorithm. *Applied Optics*, *33*, 443−452.

Guo, L. (2007). Doing battle with the green monster of Taihu lake. *Science*, *317*, 1166.

Hale, G. M., & Querry, M. R. (1973). Optical constants of water in the 200 nm to 200 μm wavelength region. *Applied Optics*, *12*, 555−563.

Hu, C., Lee, Z., Ma, R., Yu, K., Li, D., & Shang, S. (2010). Moderate Resolution Imaging Spectroradiometer (MODIS) observations of cyanobacteria blooms in Taihu Lake, China. *Journal of Geophysical Research*, *115*, C04002. doi:10.1029/2009JC005511

IOCCG (2010). Atmospheric Correction for Remotely-Sensed Ocean-Colour Products. In Wang, M. (Ed.), *Reports of International Ocean-Color Coordinating Group, No. 10, IOCCG, Dartmouth, Canada*.

Jiang, X., Tang, J., Zhang, M., Ma, R., & Ding, J. (2009). Application of MODIS data in monitoring suspended sediment of Taihu Lake, China. *Chinese Journal of Oceanology and Limnology*, *27*, 614−620. doi:10.1007/s00343-009-9160-9

Lee, Z. P., Carder, K. L., & Arnone, R. A. (2002). Deriving inherent optical properties from water color: a multiple quasi-analytical algorithm for optically deep waters. *Applied Optics*, *41*, 5755−5772.

Li, Y., Zhang, Y., & Liu, M. (2009). Calculation and retrieval of euphotic depth of Lake Taihu by remote sensing (in Chinese). *Journal of Lake Sciences*, *21*, 165−172.

Liu, X., Wang, M., & Shi, W. (2009). A study of a Hurricane Katrina-induced phytoplankton bloom using satellite observations and model simulations. *Journal of Geophysical Research*, *114*, C03023. doi:10.1029/2008JC004934

Ma, R., Duan, H., Gu, X., & Zhang, S. (2008). Detecting aquatic vegetation changes in Taihu Lake, China using multi-temporal satellite imagery. *Sensors*, *8*, 3988−4005. doi:10.3390/s8063988

Ma, R., Tang, J., Duan, H., & Pan, D. (2009). Progress in lake water color remote sensing (in Chinese). *Journal of Lake Sciences*, *21*, 143−158.

Miller, R. L., & McKee, B. (2004). Using MODIS Terra 250 m imagery to map concentrations of total suspended matter in coastal waters. *Remote Sensing of Environment*, *93*, 259−266.

Morel, A., & Gentili, G. (1991). Diffuse reflectance of oceanic waters: its dependence on sun angle as influenced by the molecular scattering contribution. *Applied Optics*, *30*, 4427−4438.

Morel, A., Huot, Y., Gentili, B., Werdell, P. J., Hooker, S. B., & Franz, B. A. (2007). Examining the consistency of products derived from various ocean color sensors in

open ocean (Case 1) waters in the perspective of a multi-sensor approach. *Remote Sensing of Environment*, *111*, 69−88.
Mueller, J. L. (2000). SeaWiFS algorithm for the diffuse attenuation coefficient, K(490), using water-leaving radiances at 490 and 555 nm, SeaWiFS Postlaunch Technical Report Series. In S. B. Hooker, & E. R. Firestone (Eds.), *NASA Tech. Memo. 2000-206892*, *Vol. 11*. (pp. 24−27) Greenbelt, Maryland: NASA Goddard Space Flight Center.
Mueller, J. M., & Fargion, G. S. (2002). Ocean optics protocols for satellite ocean color sensor validation, Revision 3, Part I & II. *NASA Tech. Memo. 2002-210004*. (pp. 1−308) Greenbelt, Maryland: NASA Goddard Space Flight Center.
Nezlin, N. P., DiGiacomo, P. M., Diehl, D. W., Jones, B. H., Johnson, S. C., Mengel, M. J., Reifel, K. M., Warrick, J. A., & Wang, M. (2008). Stormwater plume detection by MODIS imagery in the southern California coastal ocean. *Estuarine, Coastal and Shelf Science*, *80*, 141−152.
O'Reilly, J. E., Maritorena, S., Mitchell, B. G., Siegel, D. A., Carder, K. L., Garver, S. A., Kahru, M., & McClain, C. R. (1998). Ocean color chlorophyll algorithms for SeaWiFS. *Journal of Geophysical Research*, *103*, 24937−24953.
O'Reilly, J. E., Maritorena, S., Siegel, D. A., O'Brien, M. C., Toole, D., Mitchell, B. G., Kahru, M., Chavez, F. P., Strutton, P., Cota, G. F., Hooker, S. B., McClain, C. R., Carder, K. L., Muller-Karger, F., Harding, L., Magnuson, A., Phinney, D., Moore, G. F., Aiken, J., Arrigo, K. R., Letelier, R., & Culver, M. (2000). Ocean Color Chlorophyll a Algorithms for SeaWiFS, OC2 and OC4: Version 4, SeaWiFS Postlaunch Technical Report Series. In S. B., & E. R. (Eds.), *NASA Tech. Memo. 2000-206892*Greenbelt, Maryland: NASA Goddard Space Flight Center.
Roesler, C. S., & Perry, M. J. (1995). In situ phytoplankton absorption, fluorescence emission, and particulate backscattering spectra determined from reflectance. *Journal of Geophysical Research*, *100*, 13279−13294.
Roesler, C. S., Perry, M. J., & Carder, K. L. (1989). Modeling in situ phytoplankton absorption from total absorption spectra in productive inland marine waters. *Limnology and Oceanography*, *34*, 1510−1523.
Shi, W., & Wang, M. (2007a). Observations of a Hurricane Katrina-induced phytoplankton bloom in the Gulf of Mexico. *Geophysical Research Letters*, *34*, L11607. doi:10.1029/2007GL029724
Shi, W., & Wang, M. (2007b). Detection of turbid waters and absorbing aerosols for the MODIS ocean color data processing. *Remote Sensing of Environment*, *110*, 149−161.
Shi, W., & Wang, M. (2008). Three-dimensional observations from MODIS and CALIPSO for ocean responses to cyclone Nargis in the Gulf of Martaban. *Geophysical Research Letters*, *35*, L21603. doi:10.1029/2008GL035279
Shi, W., & Wang, M. (2009a). Satellite observations of flood-driven Mississippi River plume in the spring of 2008. *Geophysical Research Letters*, *36*, L07607. doi:10.1029/2009GL037210
Shi, W., & Wang, M. (2009b). Green macroalgae blooms in the Yellow Sea during the spring and summer of 2008. *Journal of Geophysical Research*, *114*, C12010. doi:10.1029/2009JC005513
Shi, W., & Wang, M. (2009c). An assessment of the black ocean pixel assumption for MODIS SWIR bands. *Remote Sensing of Environment*, *113*, 1587−1597.
Shi, W., & Wang, M. (2010a). Satellite observations of the seasonal sediment plume in central East China Sea. *Journal of Marine Systems*, *82*, 280−285. doi:10.1016/j.jmarsys.2010.06.002
Shi, W., & Wang, M. (2010b). Characterization of global ocean turbidity from Moderate Resolution Imaging Spectroradiometer ocean color observations. *Journal of Geophysical Research*, *115*, C11022. doi:10.1029/2010JC006160
Siegel, D. A., Wang, M., Maritorena, S., & Robinson, W. (2000). Atmospheric correction of satellite ocean color imagery: the black pixel assumption. *Applied Optics*, *39*, 3582−3591.
Son, S., & Wang, M. (2009). Environmental responses to a land reclamation project in South Korea. *EOS Transactions of the American Geophysical Union*, *90*, 398−399.
Son, S., Wang, M., & Shon, J. (2010). Satellite observations of optical and biological properties in the Korean dump site of the Yellow Sea. *Remote Sensing of Environment*. doi:10.1016/j.rse.2010.10.002
Tang, J., Tian, G., Wang, X., Wang, X. M., & Song, Q. (2004). The methods of water spectra measurement and analysis I: Above water method (in Chinese). *Journal of Remote Sensing*, *8*, 37−44.
Wang, M. (1999). A sensitivity study of SeaWiFS atmospheric correction algorithm: Effects of spectral band variations. *Remote Sensing of Environment*, *67*, 348−359.
Wang, M. (2006). Effects of ocean surface reflectance variation with solar elevation on normalized water-leaving radiance. *Applied Optics*, *45*, 4122−4128.
Wang, M. (2007). Remote sensing of the ocean contributions from ultraviolet to near-infrared using the shortwave infrared bands: simulations. *Applied Optics*, *46*, 1535−1547.
Wang, M., Knobelspiesse, K. D., & McClain, C. R. (2005). Study of the Sea-Viewing Wide Field-of-View Sensor (SeaWiFS) aerosol optical property data over ocean in combination with the ocean color products. *Journal of Geophysical Research*, *110*, D10S06. doi:10.1029/2004JD004950
Wang, M., & Shi, W. (2005). Estimation of ocean contribution at the MODIS near-infrared wavelengths along the east coast of the U.S.: Two case studies. *Geophysical Research Letters*, *32*, L13606. doi:10.1029/2005GL022917
Wang, M., & Shi, W. (2008). Satellite observed algae blooms in China's Lake Taihu. *EOS Transactions of the American Geophysical Union*, *89*, 201−202. doi:10.1029/2008EO220001
Wang, M., Son, S., & Harding, L. W. J. (2009a). Retrieval of diffuse attenuation coefficient in the Chesapeake Bay and turbid ocean regions for satellite ocean color applications. *Journal of Geophysical Research*, *114*, C10011. doi:10.1029/2009JC005286
Wang, M., Son, S., & Shi, W. (2009b). Evaluation of MODIS SWIR and NIR-SWIR atmospheric correction algorithm using SeaBASS data. *Remote Sensing of Environment*, *113*, 635−644.
Wang, M., Tang, J., & Shi, W. (2007). MODIS-derived ocean color products along the China east coastal region. *Geophysical Research Letters*, *34*, L06611. doi:10.1029/2006GL028599
Zhang, Y., Qin, B., Zhu, G., Gao, G., Luo, L., & Chen, W. (2006). Effect of sediment resuspension on underwater light field in shallow lakes in the middle and lower reaches of the Yangtze River: A case study in Longgan Lake and Taihu Lake. *Science in China: Series D Earth Sciences Supp. I*, *49*, 114−125.
Zhang, B., Shen, Q., Li, J., Zhang, H., & Wu, D. (2009). Retrieval of three kinds of representative water quality parameters of Lake Taihu from hyperspectral remote sensing data (in Chinese). *Journal of Lake Sciences*, *21*, 182−192.
Zhang, M., Tang, J., Dong, Q., Song, Q., & Ding, J. (2010). Retrieval of total suspended matter concentration in the Yellow and East China Seas from MODIS imagery. *Remote Sensing of Environment*, *114*, 392−403.